The Multi-diffusion Domain Model: Past, Present and Future

T. Mark Harrison and Oscar M. Lovera

Department of Earth and Space Sciences
University of California, Los Angeles, CA 90095

Abstract. It is axiomatic that application of closure theory – the foundation of isotope-based thermochronology – requires an empirical diffusion model. Thus it is surprising that the majority of thermochronological studies have not met this requirement. The advent of the multi-diffusion domain (MDD) model transcended this limitation yielding both diffusion and age information via routine $^{40}Ar/^{39}Ar$ step-heating of K-feldspar. Observed correlations between age and Arrhenius spectra show that Ar diffusion occurs by the same mechanisms in nature as in the laboratory. Under certain conditions, these data permit the recovery of a unique, cooling history. The community reaction included some unproductive lines of argument but some stimulated refinements of the MDD model that benefited the development of thermochronology. The MDD model was recently applied to muscovite upon recognition that the same diffusion mechanism operates in vacuum step-heating as in nature. The advent of ^{40}K-^{40}Ca closure profile dating opens up a new thermochronological approach. Initial results confirm that muscovite intragrain defects can restrict effective diffusion lengthscales in white micas from 10-100s of microns. Our hope for the future of the MDD model is that it be subject to aggressive and skeptical testing by the community in which quantification is valued over assertion.

Introduction

As early as ca. 1964, geochronologists recognized that most mineral dates did not reflect rock forming ages but rather corresponded to a 'blocking' temperature at which the daughter product became stabilized (e.g., Jäger and Niggli, 1964). At about the same time, the $^{40}Ar/^{39}Ar$ variant of

K-Ar geochronology was being developed for dating meteorites (Merrihue, 1965; Merrihue and Turner et al., 1966); this approach would later come to have tremendous application in revealing terrestrial thermal histories. The advent of closure theory (Dodson, 1973) was slow to be appreciated but, by the late 1970s, sufficient confidence in this interpretation led to a new kind of diagram in which K-Ar, Rb-Sr and fission track ages were plotted against assumed closure temperatures (T_c) to infer first order rock thermal histories (e.g., Mattinson, 1978; Harrison, 1977). These early studies led to efforts to link such *T-t* histories to physical models involving magmatism, denudation and uplift (e.g., Harrison and Clarke, 1979) and exploration of the benefits of the $^{40}Ar/^{39}Ar$ step-heating method (e.g., Berger et al., 1979). The limitations of this approach soon began to become apparent, particularly the inherent insensitivity of the bulk T_c approach and paucity of reliable kinetic data which prevented accurate closure temperatures with robust uncertainties from being defined. Thus the scene was set for a transcendental approach that would simultaneously exploit the full thermochronological signal available within intracrystalline isotopic variations and provide sample-specific kinetic parameters.

In 1987, Zeitler noted that the seemingly anomalous behaviour in both $^{40}Ar/^{39}Ar$ age spectra and the associated ^{39}Ar Arrhenius plots obtained as a by-product of dating K-feldspars could be qualitatively explained by the presence of a range of effective grain sizes. Later, Lovera et al. (1989) presented a complete inversion theory under the assumption that K-feldspar comprise a distribution of diffusion domain sizes, enabling not only the quantitative calculation of the diffusion parameters but also the recovery of continuous temperature-time (*T-t*) histories ushering in an era of high resolution thermal history analysis.

K-feldspar is ideal in this role as it is widespread, potassium-rich, and, apart from alkali interdiffusion, stable during laboratory heating up to temperatures near its pre-melting point

(~1100°C). As noted, the two distinct sources of information from an $^{40}Ar/^{39}Ar$ step-heating experiment are the age spectrum and the Arrhenius plot. The age spectrum is calculated from the flux of radiogenic argon ($^{40}Ar^{*}$) relative to the reactor produced argon ($^{39}Ar_K$) that is released during discrete laboratory heating steps. The Arrhenius plot is derived by plotting diffusion coefficients (calculated from inversion of the ^{39}Ar release function assuming a single diffusion length scale) against the inverse absolute temperature of laboratory heating.

Before we continue, we note that although the concept of simultaneously degassing diffusion domains of differing size is relatively simple, there are several non-intuitive consequences for interpreting Arrhenius diagrams from step-heating data worth pointing out. Thus we offer a simple symbolic model showing the basic elements of multi-diffusion domain (MDD) behaviour. Figure 1 is a cartoon of the degassing of a sample with two widely separated diffusion domain sizes. Cross sections through the initially filled spheres (Fig. 1a) are shown as uniformly black but tend towards light gray as the diffusing gas is lost from the solid at the surface. As gas is lost, the smaller domains rapidly become exhausted (Fig. 1b) and are eventually completely degassed (Fig. 1c) while the single large domain still retains a substantial portion of its reservoir in regions most remote from the surface. Eventually, even the large domain is completely degassed (Fig. 1d).

Note that while both diffusion domain sizes contribute during the initial stages of degassing (Fig. 1b), the smaller domains dominate that mixture and thus the apparent D/r^2 (where D is diffusion coefficient and r is the domain radius) calculated from a solution of the diffusion equation (which explicitly assumes a single value of r; Crank, 1975) plots on an Arrhenius diagram as a single effective domain of size r_o, between the two domain sizes but closer to the smaller domain size (a in Fig. 1e). As the small domains become degassed, the apparent D/r^2

drops onto the Arrhenius relationship for the larger domain and now accurate reflects the kinetic properties of the larger domain size (b in Fig. 1e). An unusual aspect of simultaneous degassing a mixture of diffusion domain sizes by step-heating is that the form of the calculated Arrhenius plot is not an intrinsic property of the system but rather changes substantially depending on laboratory heating schedule (see Fig. 1 in Lovera et al., 1991). For example, the inflection in the gray curve in Figure 1e could be shifted up or down parallel to the slope of the domains by respectively shortening and lengthening the duration of laboratory heating steps, as well as causing substantial changes to the form of that curve. A good illustration of this is shown in Figure 1 of Lovera et al. (1991).

Now consider the case of a sample comprising three spherical diffusion domains of equal volume fraction that differ in radii in the proportions 1:0.1:0.01 (Fig. 2). The model Arrhenius plot (Fig. 2a) is calculated from ^{39}Ar loss in the laboratory over hours to days whereas the ^{40}Ar/^{39}Ar age spectrum (right y-axis in 2b) reflects ^{40}Ar ingrowth during linear cooling from 80 to 20 Ma. Because the shape of the Arrhenius plot varies with laboratory heating schedule for samples containing a distribution of diffusion domain sizes, an alternate form of data display termed the log (r/r_o) plot is often used (Richter et al. 1991; Fig. 1b, left y-axis). Log(r/r_o) spectra are constructed by plotting the deviation of the measured diffusivities (D/r^2) from a reference diffusion law ($D/r_o^2 = D_o/r_o^2 \cdot e^{-E/RT}$; i.e., the linear array defined in the earliest phase of degassing) at a given temperature T as a function of cumulative %^{39}Ar released (Fig. 1c). Because the intrinsic diffusivity D from the reference diffusion law is arbitrarily assigned to the sample, the log(r/r_o) value is given simply by the expression $0.5 \cdot (\log D/r_o^2 - \log D/r^2)$.

In general, basement K-feldspars yield ^{40}Ar/^{39}Ar age spectra, Arrhenius, and log(r/r_o) plots that are inconsistent with the presence of a single diffusion dimension. For example, rather than

yielding a linear array, K-feldspar Arrhenius plots show complex departures from an initial straight line segment (i.e., D/r_o^2). Although this behavior was initially thought to reflect laboratory artifacts (Harrison and McDougall, 1982), it almost certainly reflects, at least in part, the presence of discrete Ar retentivities within K-feldspar. While this could potentially be due to sites of differing energetics or even nested diffusion domains, we interpreted this behavior to reflect the presence of varying sized domains (Lovera et al., 1989).

As an example of actual sample behavior, consider perthitic K-feldspar N-13 (Harrison et al. 2000). The age (left axis) and log (r/r_o) spectra (right axis) for this sample are shown in Fig. 3a. Note that the two spectra are highly correlated (see Lovera et al., 2002), particularly over the interval of gas release between the disappearance of low-temperature Cl-correlated excess ^{40}Ar ($^{40}Ar_{XS}$) and the onset of melting above 1100°C. As will be discussed further, this is characteristic of about 70% of basement K-feldspars. Figure 3b shows the Arrhenius plot of N-13 K-feldspar with reference Arrhenius law (in grey) defined by initial gas release and Fig. 3c is the recovered thermal history. Note that this method provides continuous thermal history segments rather than a single temperature-time (T-t) datum.

Merits of the MDD Model

The original MDD model (Lovera et al., 1989) provided an internally consistent explanation for observed laboratory Ar release from K-feldspar but it wasn't until more complicated laboratory heating schedules (forward and backward cycling experiments) were initiated (Lovera et al., 1992) that the irreversible nature of the various Ar retentivities became clear. The MDD model was found to faithfully mimic the gas released at temperatures below the onset of melting (~1100°C), although the presence of small variations in activation energy cannot be ruled out (Harrison et al., 1991). Note that other competing models, such as the Multi-path model (Lee,

120 1995) discussed later, requires extra annealing assumptions to explain the K-feldspar result from
121 cycling experiments.

122 A turning point came when Lovera et al. (2002) defined a cross-correlation coefficient
123 (C_{fg}) that quantified the observed relationship between the age spectrum and the laboratory
124 diffusion properties (imaged by the $\log(r/^{r}_{o})$ plot). The cross-correlation between continuous
125 functions is extensively used in many areas of science and engineering to measure similarity; it is
126 defined by the integration of the product of such functions over the domain of interest. When it
127 is normalized by the square root of the multiplication of both integrations of the square of each
128 function, its maximum value of one is reached only when both functions are proportional over
129 the domain of interest (see Section 3 in Lovera et al., 2002, for definition of the age and $\log(r/r_o)$
130 functions and the interval of integration). Using this approach, they found high degrees of
131 correlation (e.g., C_{fg} = 0.99 in Fig. 3a) in most basement K-feldspars (those >70% of samples
132 unaffected by low temperature recrystallization or high temperature Ar_{XS}). The MDD model
133 correctly predicts that, under slow monotonic cooling, the shape of an age spectrum which
134 typically represents the accumulation of ^{40}Ar over millions of years) should contain within it the
135 form of the convolved degassing of ^{39}Ar from multiple domains in the laboratory (data generated
136 over the course of only a matter of hours).

137 The MDD model also provides two clear indicators that annealing does not significantly
138 affect K-feldspar Ar that is released below the onset of melting. The first is that $\log(r/r_o)$ plots
139 are quite independent of the heating schedule used (cycling vs. monotonic experiments). Despite
140 uncertainties in the domain distribution between samples, quite similar $\log(r/r_o)$ plots were
141 obtained from the same K-feldspar applying quite different heating schedules, although as
142 expected, the same reproducibility is obtained for the age spectra (Lovera et al., 1991). Another

indicator of the low incidence that annealing effects have on the laboratory K-feldspar Ar release was obtained during a double-irradiation experiment carried out on the MH-10 K-feldspar (Lovera, et al., 1993). After degassing an aliquot of MH-10 K-feldspar using heating steps between 450-850°C to exhaust the smallest domains in the sample, it was sent back to the reactor to replenish Ar in those domains. Applying the same heating schedule on the re-irradiated sample reproduced the previous ^{39}Ar degassing demonstrating that the kink observed at temperatures above 700°C was not due to annealing effects on the sample but to the exhaustion of the argon gas in the less retentive sites. Lastly, the relative (~1000:1) and absolute sizes of the discrete Ar retentivities inferred from basement K-feldspars (ca. 100 to 0.1 μm) are in broad agreement with the range of observed microstructural features from regions of unaltered 'tweed' feldspar (ca. 100s of μm) to perthite lamellae approaching the ^{39}Ar recoil limit (ca. 0.1 μm) (Fitz Gerald and Harrison, 1993).

With the advantage of nearly 10 years of experience with the MDD model, Lovera et al. (1997) evaluated a large database (n = 115) of ^{40}Ar/^{39}Ar analyses of K-feldspars and found remarkably systematic behavior in terms of the kinetic data obtained from measured ^{39}Ar loss. Variations in apparent activation energy from a canonical value of 46 kcal/mol could be attributed to sample-specific limitations (e.g., non-uniform K distributions, insufficient mass of the smaller domain sizes to resolve r_o). Nonetheless, they showed that a misestimate in E is broadly compensated by an increase in the apparent frequency term thus buffering against substantially misestimated thermal histories. This paper appears to have been influential in the thermochronological community – possibly because of the emphasis on the behavior of real samples over mathematical theory – as an increasing number of studies from other groups began to corroborate the self-consistency of the MDD method in determining coherent, internally

166 consistent cooling histories, from both multiple coexisting K-feldspars and results obtained from
167 other well developed thermochronometric methods (i.e., apatite fission track, (U+Th)/He zircon
168 and apatite, $^{40}Ar/^{39}Ar$ biotite and muscovite, etc.; Warnock & Zeitler, 1998; Axen et al., 2000;
169 Spell et al., 2000; Kirby et al., 2002; Reiners and Farley, 1999; Reiners et al., 2004, Shirvell et
170 al., 2009). Important advances in the understanding of the tectonics of the Himalaya and
171 Peninsula Ranges, Baja California were possible through the application of the MDD model to
172 an increasingly large database of K-feldspar analyses (Quidelleur et al., 1997; Harrison et al.,
173 1995; Harrison et al., 2000; Grove et al, 2003).

174 Several notable advancements of the MDD model have been made over the two decades
175 since its introduction. The development of a Cl-correction method to remove Ar_{XS} effect at the
176 beginning of the age spectrum of contaminated samples (Harrison et al., 1994) permitted use of a
177 significant fraction of K-feldspars for thermochronology that were affected by low-temperature
178 Ar_{XS}. Incidentally, the isothermal heating steps systematically performed at low-temperature
179 (<700°C) to carry out the Cl correction (Harrison, et al., 1994) was key to probe the robustness
180 of the linear array that determine the activation energy and to understanding the meaning of
181 anomalously low apparent Ar retentivities (Lovera et al., 1997).

182 Development of automatic routines to invert the $^{40}Ar/^{39}Ar$ data, determine the sample
183 diffusion parameters, domain distribution and cooling history, incorporating at the same time the
184 propagation of the uncertainties of the diffusion parameters into the uncertainty on the final
185 determination of the cooling history helped optimize the signal to noise ratio and provided a
186 relatively user-friendly interface to the model (Lovera, 1992, Lovera et al., 1997). The
187 development of a method to measure the correlation between an age spectrum and $\log(r/r_o)$ plot
188 (Lovera et al., 2002) permitted quantitative evaluation of the correlation between both spectra to

help to identify any departures from the model hypothesis (i.e., low-temperature re-crystallization or high-temperature Ar_{XS}) that rule out ~30% of samples under consideration using the MDD model (Lovera et al., 2002).

Criticisms of the MDD Model

Despite the internally consistent predictions of the MDD model and acceptance in some quarters (e.g., Lister and Baldwin, 1996; McLaren and Dunlap, 1996; Mock et al., 1999; Sanders et al., 2006; Wang et al., 2004; Metcalf et al., 2009; Scott et al., 2009), numerous criticisms of the approach were posited during the 1990s. These critiques came in three broad themes: 1) Feldspar mineralogy precludes MDD behavior; 2) Observed ^{39}Ar release from K-feldspar is inconsistent with the MDD model; and 3) The MDD model formulation is fundamentally incorrect.

The most protracted criticism of extracting thermal history information via $^{40}Ar/^{39}Ar$ step-heating measurements came from Ian Parsons and his co-workers based on age relationships among alkali feldspars in the 1166 Ma Klokken syenite, south Greenland (e.g., Parsons et al., 1988, 1999). The prevailing view in 1988 was that the apparently low retentivity of $^{40}Ar^*$ in basement K-feldspars was due to microscale perthitic development causing a reduction in the effective diffusion dimension to the scale of the spacing of exsolution lamellae (e.g., Foland, 1974). Thus it appeared paradoxical that Parsons et al. (1988) could document pristine 'braid' micro- and cryptoperthites from the shallowly emplaced Klokken intrusion that yielded $^{40}Ar/^{39}Ar$ ages broadly similar to the emplacement age, implying little or no loss of $^{40}Ar^*$, whereas 'patch' perthites exsolved at up to the mm-scale gave much younger ages (Parsons et al., 1988; Burgess et al., 1992). Parsons et al. (1988) surmised that the turbid regions of patch perthite had lost $^{40}Ar^*$ via micropores that formed during dissolution-reprecipitation reactions whereas the braid

perthites had behaved as unitary diffusion domains despite their fine-scale microtexture. Although the timing of crystallization of these two phases had not been independently established, Parsons et al. (1988) concluded that laboratory degassing of Ar does not occur in an analogous fashion to nature, precluding the use of slowly-cooled K-feldspars for thermochronologic investigations (e.g., Harrison and McDougall, 1982).

In a series of papers over the intervening two decades, Parsons and co-workers (e.g., Burgess et al., 1992; Waldron et al., 1994; Walker et al., 1995; Parsons et al., 1999, 2010) developed their case for the inappropriateness of applying laboratory degassing data to infer K-feldspar thermal histories. They did not propose tests of the MDD model but instead arrived at conclusions that were of an absolute and assertive nature. For example, Parson et al. (1999) wrote: "Our analysis leads us to conclude that it is impossible to obtain quantitative information on cooling history from the $^{40}Ar/^{39}Ar$ spectra of microtexturally complex K-feldspars…It is our view that $^{40}Ar/^{39}Ar$ thermochronology, as applied to alkali feldspars…using the MDD method, is fundamentally flawed…We conclude that MDD thermochronology is a mirage produced by real microtexture…The apparent age spectra and Arrhenius plots do not contain extractable information on geological cooling history".

Despite numerous microscopic studies characterizing Klokken feldspars (e.g., see summary in Parsons and Lee, 2009), an additional occurrence – a near pure adularia that precipitated at very low (<200ºC) temperature – was only recently recognized (Parsons et al., 2009, 2010; Heizler et al., 2010). This low formation temperature, coupled with the relatively youthful $^{40}Ar/^{39}Ar$ ages, led Heizler et al. (2010) to conclude that some alkali feldspars in the Klokken intrusion had experienced recrystallization as late as Paleozoic time.

Harrison et al. (2010) investigated the K-Ca isotopic systematics of Klokken syenite K-feldspars and found apparent isochrons that were explained by mixing of age components ranging from crystallization to Late Proterozoic. This supported Heizler et al.'s (2010) view that the syenite had been affected by aqueous-fluid-mediated, dissolution-reprecipitation event(s) under largely closed system conditions at <200ºC, perhaps as recently as ca. 400 Ma. Prior inferences by Parsons and co-workers that the relatively young, turbid alkali feldspars had 'leaked' $^{40}Ar^*$ are in fact incorrect. Rather, partial recrystalization of these coarsely exsolved perthites to an assemblage including adularia occurred episodically many 100's of millions of years after syenite crystallization. Inferring Ar retentivity in alkali feldspars without first determining and taking account the age of the crystal microtextures proved to be an unfortunate misdirection to understanding the potential of K-feldspar for $^{40}Ar/^{39}Ar$ thermochronology.

A more generic criticism of Parsons et al. (1999) was the extent to which underlying assumptions of the MDD could apply to K-feldspars, particularly during vacuum laboratory heating. It is implicit in the above discussion that two fundamental assumptions must be satisfied to permit estimation of crustal thermal histories from K-feldspar $^{40}Ar/^{39}Ar$ step-heating data. These are: (1) that both $^{40}Ar^*$ and ^{39}Ar loss from K-feldspar are governed by volume diffusion; and (2) laboratory Ar release adequately mimics the natural diffusion boundaries and mechanisms. Failure of either of these assumptions precludes recovery of useful thermal history data. Our view is that the high degrees of correlation between the age and $\log(r/r_o)$ spectra in most of the basement K-feldspars (Lovera et al., 2002) requires that ^{40}Ar loss proceeds by volume diffusion and that laboratory Ar release must be controlled by the natural diffusion mechanisms and boundaries. By comparison, other commonly made assumptions critiqued by Parsons et al. (1999) are second order issues (i.e., uniform $^{39}Ar_K$ distribution, prescribed

diffusion geometry (slab, cylinder, sphere), zero $^{40}Ar^*$ boundary conditions, etc.) that can be dealt with by appropriately modifying the model (Lovera et al., 2002).

Lee (1995) presented an alternate kinetic model for the diffusion of Ar that followed the non-equilibrium multi-path diffusion of Ainfantis (1979). This model incorporates the combined influence of both volume and Short-Circuit (SC) diffusion (Hart, 1957). Although the Lee (1995) model was able to explain the laboratory diffusion results for some K-feldspar data generated from simple, monotonic laboratory heating schedules, it failed to predict the Ar diffusion behavior seen in cycled heating experiments (Lovera et al., 1993). Furthermore, the mechanism for mass transfer between SC and lattice (i.e., volume diffusion) reservoirs has never been physically explained.

Arnaud and Kelley (1997) tested the ability of both methods (MDD and Multi-path) to explain experimental results obtained from a gem-quality orthoclase from Madagascar that was subject to different heating schedules. Although the authors concluded that both models reproduce the data to varying degrees, the multi-path model with transfer between the SC and lattice was able to reproduce the cycling temperature results only when either the transfer was negligible (in effect reducing the model to the MDD model) or when the transfer paths were completely annealed after reaching a threshold temperature. Furthermore, the double-irradiation experiments of Lovera et al. (1993) showed that even in inhomogeneous samples (e.g., MH-10 orthoclase), annealing effects were not observed even after the sample has been subjected to a heating schedule including multiple isothermal steps of 850°C (~2 hrs), sufficient to reduce the diffusivity of the control aliquot by an order of magnitude.

A final, and fatal, shortcoming of the Multi-path diffusion model (Lee, 1995) as applied to K-feldspars is the fact that the postulated mass transfer mechanism between the SC and lattice sites

predicts no correlation between $^{40}Ar/^{39}Ar$ age (reflecting <350°C release in nature) and log(r/r_o) plots (generated from 450-1100°C release in the lab) . By contrast, most basement analyzed K-feldspars (>70%, Lovera et al. 2002) show highly correlated age and log(r/r_o) spectra indicating negligible mass interchange between hypothesized SC and lattice sites. At this limit, the Multi-path model is effectively transformed into the simpler volume diffusion MDD model. As a generalization, we conclude that the non-Fickian effects emphasized by the Multi-path model appear to be essentially absent in most basement K-feldspars. This is a non-trivial conclusion as any significant mass transfer between SC and lattice sites would effectively prevent the reconstruction of geological thermal histories using thermochronological methods.

Several studies emphasized the effect of deformation on the preservation of thermal history information in K-feldspars. For example, Reddy et al. (1999) inferred the presence of a series of undefined Ar reservoirs within K-feldspar connected via fast-diffusion pathways that they found difficult to reconcile with the MDD model. Reddy et al. (2001) further examined K-feldspars that were deformed close to the closure temperature interval and concluded that "…MDD modeling of $^{40}Ar/^{39}Ar$ data from deformed K-feldspars is fundamentally flawed and is unlikely to reproduce the actual thermal history of the sample". We agree that accurate thermal history information is unlikely to be obtained from samples that obviously violate the conservation of diffusion mechanism and boundary assumptions. Indeed, we note that the presence of such intragrain deformation microstructures imposed post-^{40}Ar-closure would almost certainly be detectable through poor correlation between their age and Arrhenius spectra (Lovera et al., 2002).

A report by Villa (1994) based on experiments performed using a granitoid K-feldspar (i.e., ga1) claimed to show Multi-path behavior. The conclusions of Villa (1994) were refuted by Lovera et al. (1996) who revealed both deep flaws in Villa's interpretation of the ga1 data and a

303 significant lack of consistency and reproducibility between data presented in Villa (1994) and
304 that reported in a previous step-heating ^{39}Ar experiment of ga1 (Villa, 1990).

305 Concerns about the effect of nuclear recoil, during the production of ^{40}Ar and ^{39}Ar from the
306 spontaneous or neutron induced decay of K were raised by Onstott et al. (1995) and Villa (1997).
307 However, the scale of ^{39}Ar recoil inferred by Villa (1997) of 0.08 μm (virtually identical to that
308 determined earlier by Turner and Cadogan (1974) is consistent with the characteristic scale of the
309 smallest resolvable diffusion domains in K-feldspars (~0.1 μm; Lovera et al., 1993; McDougall
310 and Harrison, 1999). Although there is no evidence that ^{39}Ar recoil loss significantly effects the
311 MDD thermochronology, we note that the smallest domains usually comprise only a few percent
312 (1-3%) of the sample volume and that Ar released from this zone is the most susceptible to
313 excess of argon contamination, thus usually given rise to the less reliable temperature constrains.

314 Foland (1994) undertook bulk loss and step-heating results of gem-quality Benson Mines
315 orthoclase and invoked a variety of mechanisms (e.g., synheating grain fracturing, defect
316 trapping of argon, annealing at high temperatures) to reconcile seeming differences between
317 results of long-term, isothermal Ar loss experiments and step-heating of irradiated specimens.
318 However, Lovera et al. (1997) showed that Benson Mines orthoclase ^{39}Ar bulk loss and
319 $^{40}Ar/^{39}Ar$ step heating data (Foland, 1974, 1994, Foland and Xu 1990) are consistent with a
320 modest distribution of diffusion domains sizes. Despite its gem-like nature, Benson Mines
321 orthoclase appears to contain a mosaic of internal diffusion boundaries (possibly due to a fractal
322 distribution of surface irregularities) that endow this sample with minor multi-diffusion domain
323 properties. At the least, MDD theory provides a more consistent and simpler explanation of the
324 data than that proposed by Foland (1994).

Ten years have elapsed since the demonstration that highly correlated age and Arrhenius spectra can separate those samples appropriate for MDD modeling from those that are not (Lovera et al., 2002), and nearly two since the premise of Klokken feldspar stability (Parsons et al., 1988, 1999) was proven wrong (Harrison et al., 2010). How far has the community come in moving beyond invalid criticisms of the MDD model (e.g., Parsons et al)? By some measures, perhaps not very. For example, Flude et al. (2012) conclude an otherwise interesting paper with the statement: "Another criticism of the MDD model is that the microtextures of importance to the model may actually form below the closure T for argon diffusion (Parsons et al. 1999)".

Present and Future of the MDD Model

K-Ar Muscovite MDD Thermochronology

The hydrothermal diffusion study of Ar in muscovite of Harrison et al. (2009) yielded a linear Arrhenius array indicative of $^{40}Ar^{*}$ transport by volume diffusion (E = 64 kcal/mol, log D_o = 2.3 cm^2/sec). Surprisingly, $^{40}Ar/^{39}Ar$ degassing of the treated material showed the distinctive form of samples that had been outgassed via diffusion despite the potential for decomposition of the hydrous phase in vacuum. Furthermore, they found that the age and log(r/r_o) spectra for the hydrothermally treated muscovite samples showed a remarkable degree of correlation indicating that muscovite can retain the Ar diffusion boundaries and mechanisms that define their natural retentivity during vacuum step heating. Even more surprising, Harrison et al. (2009) found that Arrhenius parameters essentially identical to that found in the hydrothermal study could be reproduced from the *in vacuo* data alone.

Heizler and Harrison (2009) undertook sizing experiments which showed that the highest retentivity in muscovite is sized controlled ($r \leq 125$ μm) and, from log(r/r_o) plots, that the smallest observable diffusion size was order ~1 μm. It thus appears that, like K-feldspars, Ar

348 release from muscovite can proceed in vacuo by diffusion and that ^{40}Ar loss in Nature may also
349 be defined by same boundaries and mechanisms as in the laboratory.

350 As an illustration of this approach, we undertook MDD modeling on ^{40}Ar/^{39}Ar results for a
351 fine-grained ($r \approx 100$ μm) muscovite separate from phylite sample AR08 in the footwall of the
352 Main Cetral Thrust, Nepali Himalaya, that cooled through Ar closure during the late Tertiary
353 (Haviv et al., 2012). The age spectrum (Fig. 6a) rises from ~12 to 20 Ma over ~75% of the gas
354 release with the initial and last portions of the spectrum contaminated with extraneous ^{40}Ar. The
355 relatively small volume fraction of the smaller diffusion domains precludes independent
356 determination of E from the Arrhenius plot (Fig. 6b), but using the value determined for
357 hydrothermal and in vacuo studies (E = 64 kcal/mol Harrison et al., 2009) yields a thermal
358 history (Fig. 6c) consistent with a large regional dataset (Haviv et al,. 2012). A test of the
359 efficacy of using the 64 kcal/mol activation energy is whether the $\log(r/r_o)$ plot shows correlated
360 inflections. Visual inspection of the two spectra (Fig. 6a) shows a clear relationship which is
361 quantitatively confirmed by a correlation coefficient (C_{fg}) of 0.93 over 83% of the spectra
362 (Lovera et al., 2002).

363 Collectively, these observations have tremendous potential for significantly diversifying high
364 resolution ^{40}Ar/^{39}Ar thermochronology as muscovite is highly retentive of Ar and widespread in
365 the continental crust.

366 *K-Ca Muscovite MDD Thermochronology*

367 The decay of ^{40}K to ^{40}Ar forms the basis of the K-Ar dating method, but only one out of
368 every ten parent atoms decays to ^{40}Ar (McDougall and Harrison, 1999). The other 90% decay to
369 ^{40}Ca giving, in principle, the ^{40}K-^{40}Ca decay system considerable potential for dating
370 Precambrian samples with high K/Ca (e.g., Marshall and DePaolo, 1982; Shih et al., 1994), such

as seen previously for Klokken adularia. This method, however, has been limited as an ion-microprobe-based geochronometer because of the very high mass resolving power of ~25,000 required for full separation. Harrison et al. (2010) instead developed a method using doubly-charged Ca and Ar species which has the effect of virtually completely suppressing $^{40}K^{++}$ from the mass spectrum leaving $^{40}Ca^{++}$ uninterfered. Detection of $^{39}K^{++}$ then permits $^{40}Ca/^{40}K$ (i.e., the daughter/parent ratio) to be calculated from the known $^{39}K/^{40}K$.

Using age standard muscovite U68, for which a 2550 Ma age has been determined by isotope dilution (Fletcher et al. 1997), we have explored the potential of this approach to thermochronometry. Reconnaissance traverses were made across two grains of muscovite from sample 82-315, an Archean muscovite schist from the Pilbara greenstone belt of Western Australia, using a ca. 20 μm primary O^- spot. Its 2.95 Ga $^{40}Ar/^{39}Ar$ age (Wijbrans and McDougall, 1987) makes it among the oldest known micas (see also Zegers et al., 1999). One, generally crack-free, grain shows coherent K-Ca age variations over 100s of μm lengthscales ranging from 3300 to 2800 Ma (Fig. 4a). This pattern can be interpreted to result from either slow cooling through that age interval or episodic loss at some time subsequent to ~2.8 Ga, although there is little evidence from conventional $^{40}Ar/^{39}Ar$ age dating for such a late thermal disturbance (Zegers et al., 1999).

A second grain shows billion-year age gradients at lengthscales of μm's to 10's of μm's (Fig. 4b). In some cases, these abrupt age gradients do not appear to correlate with visible cracks. Within this complex pattern, age gradients consistent – but not necessarily diagnostic – of Ca isotopic closure can be identified. For example, the region in the lower left of Fig. 4b appears to show a symmetric profile of ages ranging from 3.1 to 2.0 Ga (Fig. 5). Note that we do not expect such gradients to be uniformly expressed within a single grain. Rather, each sub-domain within

394 the crystal yields a potentially unique profile that reflects the natural diffusion boundaries. Our
395 only expectation is that each closure profile should define a segment of the unique thermal
396 history shared by all locations in that crystal. Thus, despite the very different approach from
397 MDD analysis of $^{40}Ar/^{39}Ar$ step-heating data, this method can be characterized as a multi-
398 diffusion-domain behavior.

399 We extracted thermal history information from the closure profile in Fig. 5 using:

400 $$\frac{E}{\Re T_c} = 1n\,(\gamma\,\tau\,D_0 / r^2) + 4S_2(x) \quad (1)$$

401 where γ = 1.78, $\tau = \Re T_c^2 / E \cdot dT/dt$, and $4S_2(x)$ describes the concentration distribution for
402 different geometric solutions (Dodson, 1986). Summations of $4S_2(x)$ as a function of position for
403 various diffusion geometries are given in Dodson (1986).

404 By forward modeling to equation (1), we recovered the continuous *T-t* history shown in Fig.
405 5 which indicates a monatonic cooling from ca. 310 to 300°C between 3 and 2 Ga (inset in Fig.
406 5). This history implies that even younger ages in the grain reflect closure at <300°C. While
407 this apparent cooling history illustrates the potential of the method, two significant limitations
408 remain. The first is that we do not yet have a robust diffusion law for Ca in muscovite. For the
409 present, we have assumed the same activation energy for Ca in muscovite as that determined for
410 Ar (i.e., 64 kcal/mol; Harrison et al., 2009) and coupled with a single determination of D_{Ca} at
411 600ºC of ~10^{-14} cm^2/s from which a D_o of ~200 cm^2/s can be inferred (Harrison, 2010). Note
412 that assuming a lower value of *E* results in even lower closure temperature estimates. Secondly,
413 the lateral resolution of this age profile is insufficient to uniquely interpret it as a closure – as
414 opposed to episodic loss – profile. However, as instrumental methods improve permitting even
415 smaller ion microprobe spot sizes, we anticipate achieving μm-scale spatial resolution for
416 Precambrian samples.

417 Note that the low concentrations (<50 ppm) of Ca in most white micas effectively precludes
418 exchange of $^{40}Ca^*$ with common ^{40}Ca occurring via self-diffusion. Thus the low
419 (<300°C)apparent T_c of $^{40}Ca^*$ in much of the 82-315 white mica relative to, say ^{40}Ar, might seem
420 surprising. This likely reflects both the small *r* and mobility of Ca among interlayer sites due to
421 its relatively small ionic radius (~1.1 Å). The intergranular region of the host rock provides an
422 essentially infinite sink for $^{40}Ca^*$.

423 With the advent of increasingly sensitive noble gas mass spectrometers and finely focused
424 laser heating/ablation sources, in situ $^{40}Ar/^{39}Ar$ studies of muscovites revealed widespread age
425 gradients due to a variety of mechanisms including diffusive closure, deformation and re-
426 crystallization (e.g., Reddy et al., 1996; Hames and Cheney, 1997; Hames and Hodges, 1997;
427 Kramar et al., 2001; Markley et al., 2002; Mulch et al., 2005; Wells et al., 2008). In general,
428 these studies suggest that slowly cooled white micas can behave as coherent diffusion domains at
429 lengthscales of ca. 1000 μm, although composition effects have been observed (Smith et al.
430 2005). However, one clear implication of the K-Ca profiles for $^{40}Ar/^{39}Ar$ dating is that grain size
431 does not define the diffusion domain size in these grains. In situ K-Ca profiling offers a rapid
432 and direct method to reveal Ca diffusion boundaries and lengthscales in muscovite. To the
433 extent that an extended subgrain defect acting as an exchange boundary for Ca is also likely to be
434 permeable to Ar, K-Ca age characterization of a large population of white micas should enhance
435 our understanding of the specific and effective diffusion lengthscales for diffusion white micas.

436 *Extraterrestrial materials*

437 Although the earliest application of both the $^{40}Ar/^{39}Ar$ method and the diffusion theory of age
438 spectra was to meteorite (Merrihue and Turner, 1966; Turner, 1968) and lunar samples, in many
439 respects, interpretation of extraterrestrial samples has lagged behind studies of terrestrial

440 materials. After an initial flurry of analyses in the 1970s following return of the Apollo samples
441 (see review in McDougall and Harrison, 1999), the field remained relatively quiet until the 1990s
442 when interest in the Late Heavy Bombardment (LHB) was rekindled (Dalrymple & Ryder, 1990,
443 1991, 1993, 1996; Ryder et al., 1996; Culler et al., 2000; Norman et al., 2006, 2010). The LHB
444 is the period from ~3.85 to 3.95 Ga during which an intense flux of asteroidal and cometary
445 bodies is hypothesized to have impacted bodies in the inner solar system – the clearest example
446 being the large lunar basins (Tera et al., 1974). While this hypothesis remains controversial
447 (e.g., Baldwin, 1974; Hartmann, 1975; Hartmann et al., 2000; Warren, 2004), a developing
448 theory termed the "Nice model" (Gomes et al., 2005; Morbidelli et al., 2005) provides an
449 explanation. They propose that a fundamental shift in orbital resonance among the Jovian
450 planets at ca. 3.8 Ga destabilized the disk of planetesimals in the outer solar system, resulting in
451 the scattering of these objects inwards. Thus establishing the age and/or existence of the LHB is
452 a matter of heightened importance to planetary scientists.
453 With the exception of a few recent contributions (e.g., Cassata et al., 2010; Shuster et al.,
454 2010), interpretation of $^{40}Ar/^{39}Ar$ data from fine-grained, polyphase extraterrestrial samples has
455 not been informed by developments of the MDD model. In particular, use of apparent linear
456 arrays in Arrhenius plots derived from ^{39}Ar release in step-heating experiments and unphysical
457 definitions of 'plateau' ages (see reviews in Bogard, 1995, 2011) may be hindering a clear test of
458 hypotheses, such as the LHB. With the advent of a new generation of rare gas mass
459 spectrometers with increased sensitivity, a renewed focus of $^{40}Ar/^{39}Ar$ dating of rare
460 extraterrestrial materials coupled with the interpretive advances of the past 25 years could
461 resolve the bombardment history of the inner solar system – a question designated by the U.S.

National Academy of Sciences as the number one priority goal for future lunar research (National Research Council, 2007).

Summary

K-feldspar provides an extraordinary opportunity to obtain continuous, high-resolution thermal histories by application of the multi-diffusion domain model to $^{40}Ar/^{39}Ar$ step-heating data. This approach yields two distinct sources of kinetic information (the age and Arrhenius spectra) from which quantitative measures of discrete Ar retentivity can be obtained. Provided a high correlation is observed between these two spectra, unique thermal history data can be obtained, regardless of choice of diffusion model.

The MDD model was greeted with intense skepticism from several fronts, including hypothesized mineralogical limitations, alternate models of Ar diffusion transport in silicates, and a claim of irreproducibility. It is fair to say that none of these arguments proved sustainable and that over 20 years of experience of producing internally consistent thermal histories that are corroborated by other well-developed thermochronometric methods has resulted in broad acceptance.

The application of the MDD model was recently expanded to include muscovite with recognition that both age and vacuum step-heating derived Arrhenius spectra reflect Ar release via the same diffusion mechanism. The advent of ^{40}K-^{40}Ca closure profiling confirms that natural muscovites can contain intragrain defects that restrict effective diffusion lengthscales in white micas from 10s to a few100s of microns. The best possible future of the MDD model is that it be subject to aggressive and skeptical testing by the community in which quantification is valued over assertion.

Acknowledgements

We thank Frank Richter, Marty Grove and Keith Mahon for their contributions to the development and testing of the MDD model. We thank those of our critics who inspired us to look deeper for answers to their questions. We thank Kevin McKeegan and Axel Schmidt for their roles in the development of SIMS K-Ca dating and Matt Heizler for recognizing the capacity of muscovite to yield meaningful kinetic constraints from vacuum heating data. William Cassata and Simon Kelley are thanked for their reviews of the manuscript.

References

Ainfantis, E.C. 1979. A new interpretation of diffusion in high-diffusivity paths - a continuum approach. *Acta Metallurgica,* **27**, 683-691.

Arnaud, N.O., & Kelley, S.P. 1997. Argon behavior in gem quality orthoclase from Madagascar: Experiments and consequences for geochronology. *Geochimica Cosmochimica Acta*, **61**, 3227-3255.

Axen, G.J., Grove, M., Stockli, D., Lovera, O.M., Rothstein, D.A., Fletcher, J.M., Farley, K. & Abbott, P.L. 2000. Thermal evolution of Monte Blanco Dome; low-angle normal faulting during Gulf of California rifting and late Eocene denudation of the eastern Peninsular Ranges. *Tectonics*, **19**, 197-212.

Baldwin, R.B. 1974. Was there a "terminal lunar cataclysm" 3.54 x10^9 years ago? *Icarus*, **23**, 157-166.

Berger, G.W., & York. D., & Dunlop, D.J. 1979. Calibration of Grenvillian palaeopoles by $^{40}Ar/^{39}Ar$ dating. *Nature*, **277**, 46-48.

Bogard, D.D., 1995. Impact ages of meteorites: a synthesis. Meteoritics 30, 244–268.

506 Bogard, D.D., 2011. K–Ar ages of meteorites: Clues to parent-body thermal histories. *Chemie*
507 *der Erde*, **71**, 207–226.

508 Burgess, R., Kelley, S.P., Parsons, I., Walker, F.D.L., & Worden, R.H. 1992. $^{40}Ar/^{39}Ar$ analysis
509 of perthite microtextures and fluid inclusions in alkali feldspars from the Klokken syenite,
510 South Greenland. *Earth and Planetary Science Letters*, **109**, 147-167.

511 Cassata, W.S., Shuster D.L., Renne, P.R., Weiss, B.P. 2010. Evidence for shock heating and
512 constraints on Martian surface temperatures revealed by $^{40}Ar/^{39}Ar$ thermochronometry of
513 Martian meteorites, *Geochimica et Cosmochimica Acta*, **74**, 6900-6920.

514 Crank, J. 1975. *The mathematics of diffusion*, 2nd ed. Clarendon, Oxford.

515 Culler, T.S., Becker, T.A., Muller, R.A., & Renne, P.R. 2000. Lunar impact history from
516 $^{40}Ar/^{39}Ar$ dating of glass spherules. *Science*, **287**, 1785-1788.

517 Dalrymple, G.B. & Ryder, G. 1990. Ages of Apollo-15 impact melts and lunar bombardment.
518 *Meteoritics*, 25, 355-356.

519 Dalrymple, G.B. & Ryder, G. 1991. $^{40}Ar/^{39}Ar$ ages of 6 Apollo 15 impact melt rocks by laser
520 step heating. *Geophysical Research Letters*, **18**, 1163-1166.

521 Dalrymple, G.B. & Ryder, G. 1993. $^{40}Ar/^{39}Ar$ age spectra of Apollo-15 impact melt rocks by
522 laser step-heating and their bearing on the history of lunar basin formation. *Journal of*
523 *Geophysical Research*, **98**, 13085-13095.

524 Dalrymple, G.B. & Ryder, G. 1996. Argon-40/argon-39 age spectra of Apollo 17 highlands
525 breccia samples by laser step heating and the age of the Serenitatis basin. *Journal of*
526 *Geophysical Research*, **101**, 26069-26084.Dodson, M. H. 1973. Closure temperature in
527 cooling geochronological and petrological systems. *Contrib. Mineral. Petrol*. **40**, 259-274.

528 Dodson M.H. (1986) Closure profiles in cooling systems. *In*: *Materials Science Forum*, Vol 7,
529 Trans Tech Publications, Aedermannsdorf, Switzerland, p. 145-153.

530 Fitz Gerald, J.D. & Harrison, T.M. 1993. Argon diffusion domains in K-feldspar I:
531 Microstructures in MH-10. *Contributions to Mineralogy and Petrology*, **113**, 367-380.

532 Fletcher, I.R., McNaughton N.J., Pidgeon R.T., & Rosman, K.J.R. 1997. Sequential closure of
533 K-Ca and Rb-Sr isotopic systems in Archaean micas. *Chemical Geology*, **138**, 289-301.

534 Flude, S., Lee, M.R., Sherlock, S.C. & Kelley, S.P. 2012. Cryptic microtextures and geological
535 histories of K-rich alkali feldspars revealed by charge contrast imaging. *Contributions to*
536 *Mineralogy and Petrology*, **163**, 983–994.

537 Foland, K.A. 1974. ^{40}Ar diffusion in homogeneous orthoclase and an interpretation of Ar
538 diffusion in K-feldspar. *Geochimica Cosmochimica Acta*, **38**, 151-166.

539 Foland K.A. 1994. Argon diffusion in feldspars. In Parsons, I, ed., *Feldspars and Their*
540 *Reactions*, Kluwer Academic, **421**, 415-447.

541 Foland, K.A. & Xu, X. 1990. Diffusion of ^{40}Ar and ^{39}Ar in irradiated orthoclase. *Geochimica*
542 *Cosmochimica Acta*, **54**, 3147-3158.

543 Gomes, R., Levison, H.F., Tsiganis, K., & Morbidelli, A. 2005. Origin of the Cataclysmic Late
544 Heavy Bombardment Period of the Terrestrial Planets. *Nature*, **435**, 466-469.

545 Grove, M, Lovera, O. M, & Harrison T. M (2003) Late Cretaceous cooling of the east-central
546 Peninsular Ranges Batholith (33ºN): Relationships to La Posta pluton emplacement,
547 Laramide shallow subduction, and forearc sedimentation. *Geological Society of America*
548 *Special Paper*, 374, 355-380.

549 Hames, W.E. & Hodges, K.V. 1993. Laser $^{40}Ar/^{39}Ar$ evaluation of slow cooling and episodic
550 loss of ^{40}Ar from a sample of polymetamorphic muscovite. *Science*, **261**, 1721-1723.

551 Hames, W.E. & Cheney, J.T. 1997. On the loss of $^{40}Ar^*$ from muscovite during
552 polymetamorphism. *Geochimica et Cosmochimica Acta*, **61**, 3863-3872.

553 Harrison, T.M. 1977. Fission track, potassium-argon and rubidium/strontium geochronology and
554 thermal history of the Coast Plutonic Complex, near Prince Rupert, B.C. B.Sc. (hons.)
555 Thesis, Department of Geological Sciences, University of British Columbia.

556 Harrison, T.M. 2010. Diffusion in the muscovite ^{40}K decay system. Abstract V44A-02 presented
557 at 2010 Fall Meeting, AGU, San Francisco, Calif., 13-17 Dec.

558 Harrison, T.M., Heizler, M.T. McKeegan, K.D. & Schmitt, A.K. 2010. Resolving the Klokken
559 feldspar controversy using in situ ^{40}K-^{40}Ca dating. *Earth and Planetary Science Letters*,
560 **299**, 426–433**.**

561 Harrison, T.M., Celerier, J., Aikman, A.B., Herman, J. & M.T. Heizler. 2009 ^{40}Ar diffusion in
562 muscovite. *Geochimica et Cosmochimica Acta,* **73**, 1039–1051.

563 Harrison T.M., O.M. Lovera & Heizler M.T. 1991. $^{40}Ar/^{39}Ar$ results for multi-domain samples
564 with varying activation energy. *Geochimica Cosmochimica Acta*, **55**, 1435-1448.

565 Harrison, T.M., Heizler, M.T., Lovera, O.M., Chen W., & Grove M. 1994. A chlorine
566 disinfectant for excess argon released from K-feldspar during step-heating. *Earth and*
567 *Planetary Science Letters*, **123**, 95-104.

568 Harrison, T.M., Copeland P., Kidd, W.S.F., & Lovera, O.M. 1995. Activation of the
569 Nyainqentanghla shear zone: implications for uplift of the southern Tibetan Plateau.
570 *Tectonics*, **14**, 658-676.

571 Harrison, T.M., Yin, A., Grove, M., Lovera, O.M., & Ryerson, F.J. (2000) The Zedong Window:
572 A record of superposed Tertiary convergence in southeastern Tibet. *Journal of Geophysical*
573 *Research,* **105**, 19211-19230.

574 Harrison, T.M. & Clarke, G.K.C. 1979. A model of the thermal effects of igneous intrusion and
575 uplift as applied to the Quottoon Pluton, British Columbia. *Canadian Journal of Earth*
576 *Sciences*, **16**, 411-420.

577 Harrison, T.M. & McDougall, I. 1982 The thermal significance of potassium feldspar K-Ar ages
578 inferred from $^{40}Ar/^{39}Ar$ age spectrum results. *Geochimica Cosmochimica Acta,* **46**, 1811-
579 1820.

580 Hart, E.W. 1957. On the role of dislocations in bulk diffusion. *Acta Metallurgica*, **5**, 597.

581 Hartmann, W.K., Ryder, G., Dones, L., & Grinspoon, D. 2000. The time dependent intense
582 bombardment of the primordial Earth/Moon system in *Origin of the Earth and the Moon*,
583 eds Canup R., Righter K. (University of Arizona Press, Tucson, AZ), . 805-826.

584 Hartmann, W.K. 1975. Lunar "cataclysm": A misconception? *Icarus,* **24**, 181-187.

585 Haviv, I., Avouac, J.P., Farley, K.A., Harrison, T.M., Heizler, M.T., Prabhat, N.C. & Mahéo, G.
586 (2012) Decoupling of Monsoon Precipitation and Erosion Rates along the Eastern Nepal
587 Himalaya. To be submitted to *Journal of Geophysical Research*.

588 Heizler, M.T., Parsons, I., Heizler, L.L. & Sanders, R.E. 2010. Alkali feldspar microtextures and
589 Ar release II: Reconciliation via microanalysis. Abs. Thermo2010, 12th International
590 Conference on Thermochronology, Glasgow 16-20, August, 2010, pg. 59.

591 Heizler, M.T. & Harrison, T.M. 2009. Continuous thermal histories from muscovite $^{40}Ar/^{39}Ar$
592 age spectra. *Goldschmidt Conference Abstracts,* June 21 – 26, 2009, Davos, Switzerland.

593 Hudgins, J.A., Spray, J.G., Kelley, S.P., Korotev, R.L., Sherlock, S.C. 2008. A laser probe Ar-
594 40/Ar-39 and INAA investigation of four Apollo granulitic breccias. *Geochimica et*
595 *Cosmochimica Acta*, 72, 5781-5798.

596 Jäger, E. & Niggli, E. 1964. Rubidium-Strontium-Isotopenanalysen an mineralien und gesteinen
597 des Rotondogranites und ihre geologische interpretation. *Schweizer Mineralogische und*
598 *Petrographische Mitteilungen*, **44**, 61-73.

599 Kirby, E., P.W. Reiners, M.A. Krol, K.X. Whipple, K.V. Hodges, K.A. Farley, W. Tang, and Z.
600 Chen 2002. Late Cenozoic evolution of the eastern margin of the Tibetan Plateau:
601 Inferences from $^{40}Ar/^{39}Ar$ and (U-Th)/He thermochronology. *Tectonics*, **21**, 1001,
602 doi:10.1029/2000TC001246.

603 Kramar, N., Cosca, M.A., Hunziker, J.C. 2001. Heterogeneous $^{40}Ar^*$ distributions in naturally
604 deformed muscovite: in situ UV-laser ablation evidence for microstructurally controlled
605 intragrain diffusion. + *Earth and Planetary Science Letters*, **192**, 377-388.

606 Lee, J.K.W. 1995. Multipath diffusion in geochronology. *Contributions to Mineralogy and*
607 *Petrology*, **120**, 60–82.

608 Lister, G.S. and Baldwin, S.L. 1996. Modelling the effect of arbitrary P-T-t histories on argon
609 diffusion in minerals using the MacArgon program for the Apple Macintosh.
610 *Tectonophysics*, **253**, 83-109.

611 Lovera, O.M. 1992. Computer programs to model $^{40}Ar/^{39}Ar$ diffusion data from multi-domain
612 samples. *Computers and Geosciences*, **18**, 789-813.

613 Lovera, O.M., Richter, F.M. & Harrison, T.M. 1989. $^{40}Ar/^{39}Ar$ geothermometry for slowly
614 cooled samples having a distribution of diffusion domain sizes. *Journal of Geophysical*
615 *Research*, **94**, 17917-17935.

616 Lovera, O.M., Richter, F.M. & Harrison, T.M. 1991. Diffusion domains determined by ^{39}Ar
617 release during step heating. *Journal of Geophysical Research*, **96**, 2057-2069.

618 Lovera, O.M., Heizler, M.T. & Harrison, T.M. 1993. Argon diffusion domains in K-feldspar II:
619 kinetic properties of MH-10. *Contributions to Mineralogy and Petrology*, **113**, 381-393.

620 Lovera, O.M., Harrison, T.M., & Grove, M.,1996. Comment on "Multipath Ar transport in K-
621 feldspar deduced from isothermal heating experiments" by Igor Villa. *Earth and Planetary*
622 *Science Letters*, 140, 281-283.

623 Lovera, O.M., Grove, M., Harrison, T.M., & Mahon, K.I. 1997. Systematic analysis of K-
624 feldspar $^{40}Ar/^{39}Ar$ step-heating experiments I: Significance of activation energy
625 determinations. *Geochimica Cosmochimica Acta*, **61**, 3171-3192.

626 Lovera, O.M., Grove, M., & Harrison, T.M. 2002. Systematic analysis of K-feldspar $^{40}Ar/^{39}Ar$
627 step-heating experiments II: Relevance of laboratory K-feldspar argon diffusion properties
628 to Nature. *Geochimica Cosmochimica Acta*, **66**, 1237-1255.

629 Marshall, B.D. & DePaolo, D.J. 1982. Precise age-determinations and petrogenetic studies using
630 the K-Ca method. *Geochimica Cosmochimica Acta*, **46**, 2537-2545.

631 Markley, M.J., Teyssier, C., and Cosca, M., 2002. The relation between grain size and $^{40}Ar/^{39}Ar$
632 date for Alpine white mica from the Siviez-Mischabel Nappe, Switzerland. *Journal of*
633 *Structural Geology*, **24**, 1937-1955.

634 Mattinson, J.M. 1978. Age, origin, and thermal histories of some plutonic rocks from Salinian
635 Block of California. *Contributions to Mineralogy and Petrology*, **6,** 233-245.

636 McDougall, I & Harrison, T.M. 1999. *Geochronology and thermochronology by the $^{40}Ar/^{39}Ar$*
637 *Method*. 2nd ed., Oxford University Press, New York.

638 McLaren, S. & Dunlap W.J. 1996. Use of $^{40}Ar/^{39}Ar$ K-felspar thermochronology in basin thermal
639 history reconstruction: an example from the Big Lake Suite granites, Warburton Basin,
640 South Australia. *Basin Research*, **18**, 189-203, doi: 10.1111/j.1365-
641 2117.2006.00288.x.Merrihue, C. 1965. Trace-element determinations and potassium-argon
642 dating by mass spectroscopy of neutron-irradiated samples. *Trans. Am. Geophys. Un.* **46**,
643 125 (Abstract).

644 Merrihue, C., & Turner, G. 1966. Potassium-argon dating by activation with fast neutrons.
645 *Journal of Geophysical Research*, **71**, 2852-2857.

646 Metcalf, J.R., Fitzgerald, P.G., Baldwin, S.L., Muñoz, J.A., (2009) Thermochronology of a
647 convergent orogen: Constraints on the timing of thrust faulting and subsequent exhumation
648 of the Maladeta Pluton in the Central Pyrenean Axial Zone. *Earth and Planetary Science*
649 *Letters*, **287**, 488–503.

650 Mock, C., Arnaud, N.O., & Cantagrel, J-M. 1999. An early unroofing in northeastern Tibet?
651 Constraints from $^{40}Ar/^{39}Ar$ thermochronology on granitoids from the eastern Kunlun range
652 (Qianghai, NW China). *Earth and Planetary Science Letters*, **171**, 107-122.

653 Morbidelli, A., Levison, H.F., Tsiganis, K., & Gomes. R. 2005. Chaotic capture of Jupiter's
654 Trojan asteroids in the early Solar System. *Nature*, **435**, 462-465.

655 Mulch, A., Cosca, M.A., Andresen, A. and Fiebig, J. 2005. Time scales of deformation and
656 exhumation in extensional detachment systems determined by high-spatial resolution in situ
657 UV-laser $^{40}Ar/^{39}Ar$ dating. *Earth and Planetary Science Letters,* **233**, 375-390.

658 National Research Council. 2007. *The Scientific Context for Exploration of the Moon: Final*
659 *Report*. Washington, D.C., The National Academies Press, 2007. 1.

660 Norman, M.D., Duncan, R.A., Huard, J.J. 2006. Identifying impact events within the lunar
661 cataclysm from 40Ar–39Ar ages and compositions of Apollo 16 impact melt rocks.
662 *Geochimica Cosmochimica Acta*, **70**, 6032-6049.

663 Norman, M.D., Duncan, R.A., Huard, J.J. 2010. Imbrium provenance for the Apollo 16
664 Descartes terrain: Argon ages and geochemistry of lunar breccias 67016 and 67455.
665 *Geochimica et Cosmochimica Acta,* **74**, 763–783.

666 Onstott, T.C., Miller, M., Ewing, R.C., Arnold, G.W., & Walsh, D.S. 1995. Recoil refinements:
667 Implications for the $^{40}Ar/^{39}Ar$ dating technique. *Geochimica Cosmochimica Acta*, **59**, 1821-
668 1834.

669 Parsons, I., Rex, D.C., Guise, P., & Halliday, A.N. 1988. Argon-loss by alkali feldspars.
670 *Geochimica Cosmochimica Acta*, **52**, 1097-1112.

671 Parsons, I., Brown, W.L. & Smith, J.V. 1999. $^{40}Ar/^{39}Ar$ thermochronology using alkali feldspars;
672 real thermal history or mathematical mirage of microtexture? *Contributions to Mineralogy*
673 *and Petrology*, **136**, 92-110.

674 Parsons, I. & Lee, M.R. 2009. Mutual replacement reactions in alkali feldspars I: microtextures
675 and mechanisms. *Contributions to Mineralogy and Petrology*, **157**, 641–661.

676 Parsons, I., Fitz Gerald J.D., Ivanic, T., Lee, M.R., Heizler, M.T., Heizler, L.L., & Sanders R.E.,
677 2009. Microtextural and thermal evolution of cryptoperthites, microperthites and peristerites
678 in ten-phase alkali feldspars. European Mineralogical Society, MicroAnalysis, Processes,
679 Time (MAPT), Edinburgh, UK (abstract).

680 Parsons, I., Fitz Gerald, Lee, J.K.W., Ivanic, T., & Golla-Schindler, U. 2010. Time–temperature
681 evolution of microtextures and contained fluids in a plutonic alkali feldspar during heating.
682 *Contributions to Mineralogy and Petrology*, DOI 10.1007/s00410-009-0471-9.

683 Quidelleur, X., Grove, M., Lovera, O.M., Harrison, T.M., Yin, A., & Ryerson, F.J. 1997. The
684 thermal evolution and slip history of the Renbu Zedong Thrust, southeastern Tibet. *Journal*
685 *of Geophysical Research*, **102**, 2659-2679.Reddy, S.M., Potts, G.J., & Kelley, S.P., 2001.
686 $^{40}Ar/^{39}Ar$ ages in deformed potassium feldspar: evidence of microstructural control on Ar
687 isotope systematics. *Contributions to Mineralogy and Petrology*, **141**, 186-200.

688 Reddy, S.M., Potts, G.J., Kelley, S.P. 2001. $^{40}Ar/^{39}Ar$ ages in deformed potassium feldspar:
689 Evidence for microstructural control on Ar isotope systematic. *Contributions to Mineralogy*
690 *and Petrology*, **141**, 186-200.

691 Reddy, S.M., Potts, G.J., Kelley, S.P. & Arnaud, N.O. 1999. The effects of deformation-induced
692 microstructures on intragrain $^{40}Ar/^{39}Ar$ ages in potassium feldspar. *Geology*, **27**, 363-366.

693 Reddy, S.M., Kelley, S.P. & Wheeler, J. 1996. A $^{40}Ar/^{39}Ar$ laser probe study of micas from the
694 Sesia Zone, Italian Alps: Implications for metamorphic and deformation histories. *Journal*
695 *of Metamorphic Geology*, **14**, 493 – 508.

696 Reiners, P.W. & Farley, K.A. 1999. He diffusion and (U-Th)/He thermochronometry of titanite.
697 *Geochimica Cosmochimica Acta*, **63**, 3845-3859.

698 Reiners, P.W., Spell, T.L., Nicolescu, S., and Zanetti, K.A. 2004 Zircon (U-Th)/He
699 thermochronometry: He diffusion and comparisons with $^{40}Ar/^{39}Ar$ dating. *Geochimica*
700 *Cosmochimica Acta*, **68**, 1857-1887.

701 Richter, F.M., Lovera, O.M., Harrison, T.M. & Copeland, P. 1991. Tibetan tectonics from a
702 single feldspar sample: An application of the $^{40}Ar/^{39}Ar$ method. *Earth and Planetary*
703 *Science Letters*, **105**, 266-276.

704 Ryder, G., Delano, J.W., Warren, P.H., Kallemeyn, G.W., & Dalrymple, G.B. 1996. A glass
705 spherule of questionable impact origin from the Apollo 15 landing site: Unique target mare
706 basalt. *Geochimica Cosmochimica Acta*, **60**, 693-710.

707 Sanders, R.E., Heizler, M.T. and Goodwin, L.B. 2006. $^{40}Ar/^{39}Ar$ thermochronology constrains on
708 the timing of Proterozoic basement exhumation and fault ancestry, southern Sangre de
709 Cristo Range, New Mexico. *Geological Society of America Bulletin*, 1489-1506,
710 doi:10.1130/b25857.1.

711 Scott, J.M., Cooper, A.F. Palin, J.M., Tulloch, A.J. Kula, J., Jongens, R., Spell, T.L., Pearson,
712 N.J. (2009) Tracking the influence of a tracking the influence of a continental margin on
713 growth of a magmatic arc (Fiordland, New Zealand) using thermobarometry,
714 thermochronology, and zircon U–Pb and Hf isotopes. Tectonics, 28, p. TC6007, pp. 20.

715 Shih, C.-Y., Nyquist, L.E., Bogard, D.D., & Wiesmann, H. 1994. K-Ca and Rb-Sr dating of two
716 lunar granites: Relative chronometer resetting. *Geochimica Cosmochimica Acta*, **58**, 3101–
717 3116.

718 Shirvell, C.R., Stockli, D.F., Axen, G.J., & Grove, M. 2009. Miocene-Pliocene exhumation
719 along the west Salton detachment fault, southern California, from (U-Th)/He

720 thermochronometry of apatite and zircon, *Tectonics*, 28, TC2006,
721 doi:10.1029/2007TC002172.
722 Shuster, D. L., Balco, G, Cassata, W.S., Fernandes, V.A., Garrick-Bethell, I., Weiss, B.P. 2010.
723 A record of impacts preserved in the lunar regolith, *Earth and Planetary Science Letters*,
724 **290**, 155-165. Smith, S.R., Kelley, S.P., Tindle, A.G., Breaks, F.W. 2005. Compositional
725 controls on Ar-40/Ar-39 ages of zoned mica from a rare-element pegmatite. *Contributions to*
726 *Mineralogy and Petrology*, **149**, 613-626.
727 Spell, T.L., McDougall, I., and Tulloch, A.J., 2000. Thermochronologic constraints on the
728 breakup of the Pacific Gondwana margin: The Paparoa Metamorphic Core Complex, South
729 Island, New Zealand, *Tectonics*, **19**, 433-451.
730 Tera, F., Papanastassiou, D.A., & Wasserburg, G.J. 1974. Isotopic evidence for a terminal lunar
731 cataclysm. *Earth and Planetary Science Letters*, **22**, 1-21.
732 Turner, G. 1968. The distribution of potassium and argon in chondrites. In *Origin and*
733 *distribution of the elements* (ed. L. H. Ahrens), 387-398. Pergamon, London.
734 Turner, G. 1970. Argon-40/argon-39 dating of lunar rock samples. *Science*, **167**, 466-468.
735 Turner, G. & Cadogan, P. H. 1974. Possible effects of ^{39}Ar recoil in ^{40}Ar/^{39}Ar dating.
736 *Proceedings of the 5th Lunar Science Conference* , Pergamon, 1601-1615.
737 Villa, I.M. 1990. Geochronology and excess Ar geochemistry of the Lholse Nup leucogranite,
738 Nepal, Himalaya, *Journal of Volcanology and Geothermal Research*, **44**, 89-103.
739 Villa, I.M. 1994. Multipath Ar transport in K-feldspar deduced from isothermal heating
740 experiments. *Earth and Planetary Science Letters*, **122**, 393-401.
741 Villa, I. M. 1997. Direct determination of ^{39}Ar recoil distance. *Geochimica Cosmochimica Acta*,
742 **61**, 689–91.

743 Waldron, K., Lee, M.R., & Parsons, I. 1994. The microstructures of perthitic alkali feldspars
744 revealed by hydrofluoric-acid etching. *Contributions to Mineralogy and Petrology*, **116**, 360-
745 364.

746 Walker, F.D.L., Lee, M.R. & Parsons, I. 1995. Micropores and micropermeable texture in alkali
747 feldspars: geochemical and geophysical implications. *Mineralogical Magazine*, **59**, 505-534.

748 Wang, F., Lo, C.H., Qi. L., Yeh, M.W., Wan, J., Zheng, D., & Wang, E. 2004. Onset timing of
749 significant unroofing around Qaidam basin, northern Tibet, China: constraints from $^{40}Ar/^{39}Ar$
750 and FT thermochronology on granitoids. *Journal of Asian Earth Sciences*, **24**, 59-69.

751 Warnock, A.C. & Zeitler, P.K., 1998. $^{40}Ar/^{39}Ar$ thermochronometry of K-feldspar from the KTB
752 borehole, Germany. *Earth and Planetary Science Letters*, **158**, 67-79.

753 Warren, P.H. 2004. The Moon, in *Treatise on Geochemistry*, eds Holland H.D., Turekian K.K.
754 (Elsevier, Amsterdam), 559-599.

755 Wartho, J.A., Kelley, S.P., Brooker, R.A., Carroll, M.R., Villa, I.M. and Lee, M.R. (1999) Direct
756 measurement of Ar diffusion profiles in a gem-duality Madagascar K-feldspar using the
757 ultra-violet laser ablation microprobe (UVLAMP). *Earth and Planetary Science Letters*,
758 **170**, 141-153

759 Wells, M.L., Spell, T.L., Hoisch, T.D., Arriola, T. & Zanetti, K.A. 2008. Laser-probe $^{40}Ar/^{39}Ar$
760 dating of strain fringes: Mid-Cretaceous synconvergent orogen-parallel extension in the
761 interior of the Sevier orogen. *Tectonics*, **27**, TC3012, doi:10.1029/2007TC002153.

762 Wijbrans, J.R. & McDougall. I. 1987. On the metamorphic history of an Archean granitoid
763 greenstone terrane, East Pilbara, Western Australia, using the ^{40}Ar-^{39}Ar age spectrum
764 technique. *Earth and Planetary Science Letters*, **84**, 226-242.

765 Zegers, T.E., Wijbrans, J.R. & White, S.H. 1999. $^{40}Ar/^{39}Ar$ age constraints on tectonothermal
766 events in the Shaw Area of the eastern Pilbara granite-greenstone terrain (W. Australia): 700
767 Ma of Archean tectonic evolution. *Tectonophysics*, **311**, 45-81.

768 Zeitler, P.K. 1987. Argon diffusion in partially outgassed alkali feldspars: Insights from
769 $^{40}Ar/^{39}Ar$ analysis. *Chemical Geology* (*Isotope Geoscience Section*), **65**, 167-181.

770

771

Figure Captions

Figure 1. Symbolic representation of the degassing of a two phase multi-diffusion domain sample. Cross sections through the initially filled spheres are uniformly black and progressively tend towards light gray as the diffusing gas is lost from the solid at the sphere boundaries. The two domains differ in radius by a factor of 10 and are assumed to contain equal volumes. (a) Initial uniform distribution of diffusant (i.e., ^{39}Ar) in both size domains. (b) Gas loss is limited to the periphery of the single large domain while the smaller domain size has been substantially degassed. (c) The smaller domains are now completely degassed and no longer contribute to a mixture. (d) Both large and small domains are completely degassed.

Figure 2. Synthetic example (a) Arrhenius plot calculated from ^{39}Ar loss during laboratory step-heating (b) $^{40}Ar/^{39}Ar$ age spectrum (right y-axis) resulting from a 5°C/Ma linear cooling since 100 Ma. In this example, the sample is comprised of three spherical diffusion domains that differ in radii in the proportions 1:0.1:0.01 with equal volume fractions. The $\log(r/r_o)$ plot (left y-axis) shows the Arrhenius data on a spectrum-type plot as the deviation of each D/r^2 value from the linear array produced during initial degassing.

Figure 3. Typical K-feldspar age and Arrhenius properties. (a) Age spectrum (rigth axis) and log (r/r_o) spectrum (left axis) for N-13 K-feldspar (Harrison et al. 2000). Note correlated behavior, particular over the interval of gas release between the disappearance of low-temperature Cl-correlated $^{40}Ar_E$ and the onset of melting above 1100°C. C_{fg} refers to correlation coefficient calculated by Lovera et al. (2002). (b) Arrhenius plot showing measured diffusivities, reference Arrhenius law (r_o) defined by initial gas release (see text), and sample calculation of log (r/r_o) value at 1000°C (see text).

Figure 4. (A) K-Ca age map (in Ma) of muscovite 82-315 grain, Pilbara region, WA. Age variations are documented from 3300 to 2800 Ma with age discontinuities generally related to thoroughgoing cracks. (B) Another grain of muscovite 82-31, this one showing much greater age variation with gradients of billions of years over 10s of μms. The region indicate by the red box is assumed to be due to slow cooling from ca. 3200 to 2000 Ma and the apparent closure profile is modeled in Fig. 5 to obtain the thermal history shown in the inset of Fig. 5.

Figure 5. Age profile taken from the red box in Fig. 4B. The two nearly coincident model thermal histories shown in the inset (light and dark gray) differ by only 3°C yet correspond to the age profiles bounding the observed data (light and dark gray parabolas) which differ by up to 200 Ma underscoring the high sensitivity of this approach. By comparison, the K-Ar age of this sample is 2.95 Ga (Wijbrans and McDougall, 1987).

Figure 6. $^{40}Ar/^{39}Ar$ results for Himalayan muscovite AR08: (a) age and $\log(r/r_o)$ spectra, (b) Arrhenius plot and (c) thermal history derived from inversion of data in (a) and (b). The correlated inflections between the age and $\log(r/r_o)$ spectra is evidence that the conservation of diffusion mechanism and boundary assumption is met despite the metastable nature of muscovite during vacuum heating.

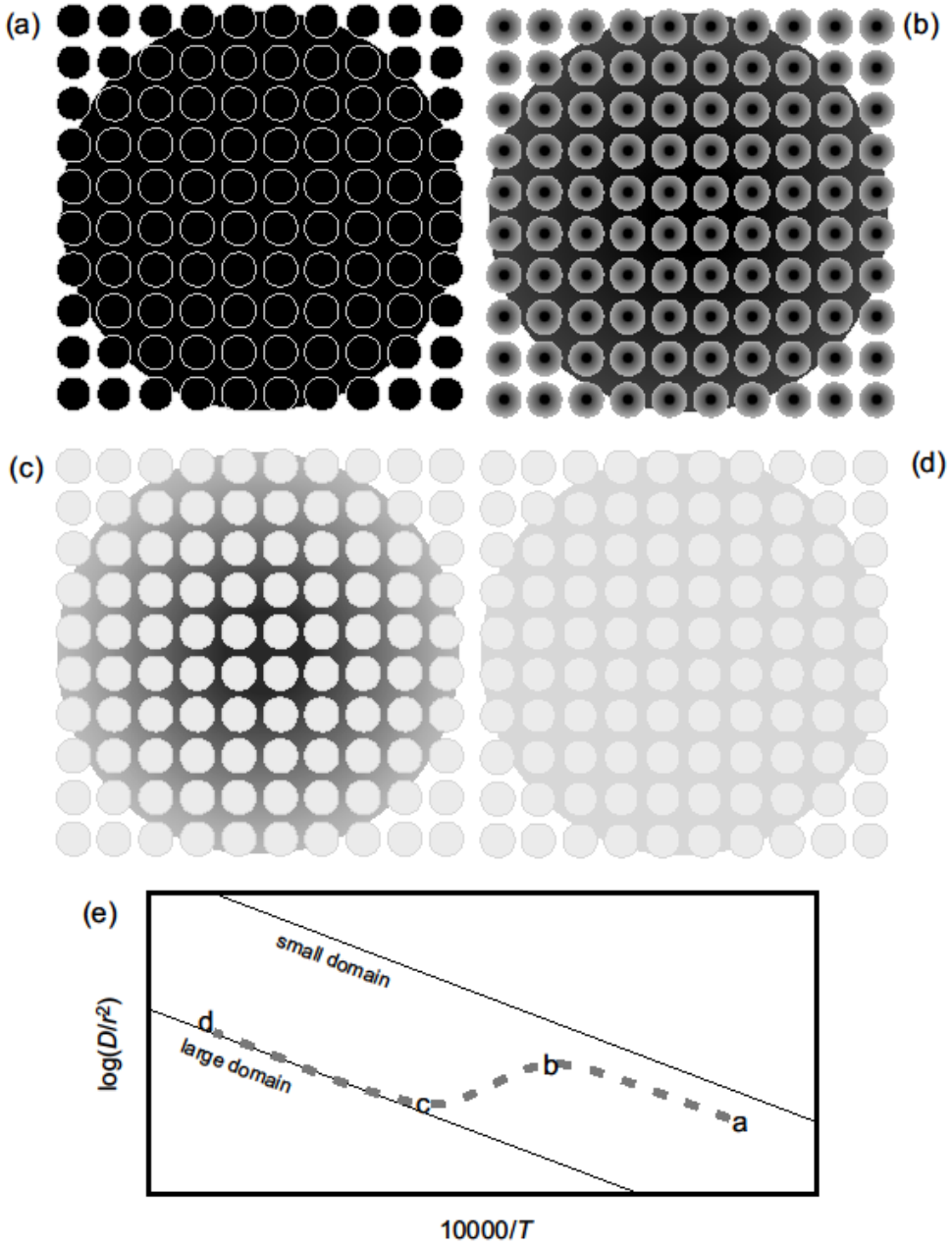

Figure 1.

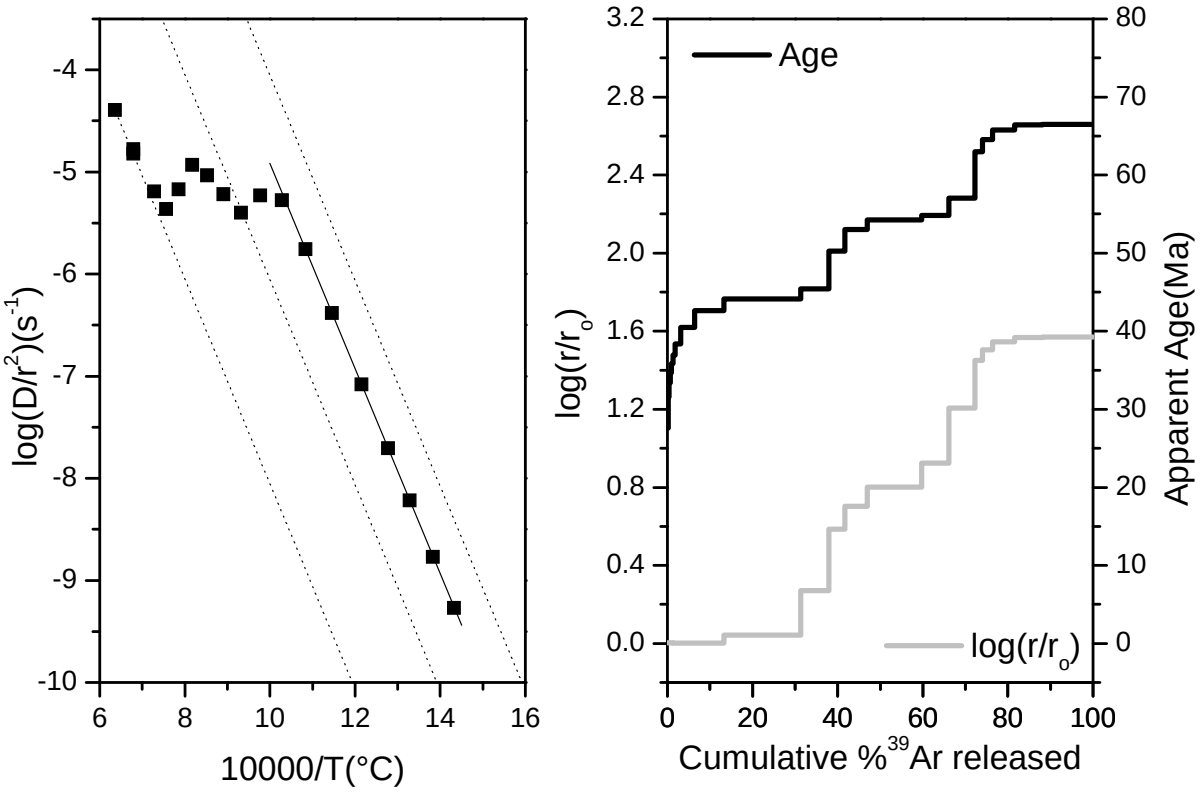
log(D/r²)(s⁻¹)
10000/T(°C)
log(r/r_o)
Apparent Age(Ma)
Age
log(r/r_o)
Cumulative %³⁹Ar released

Figure 2.

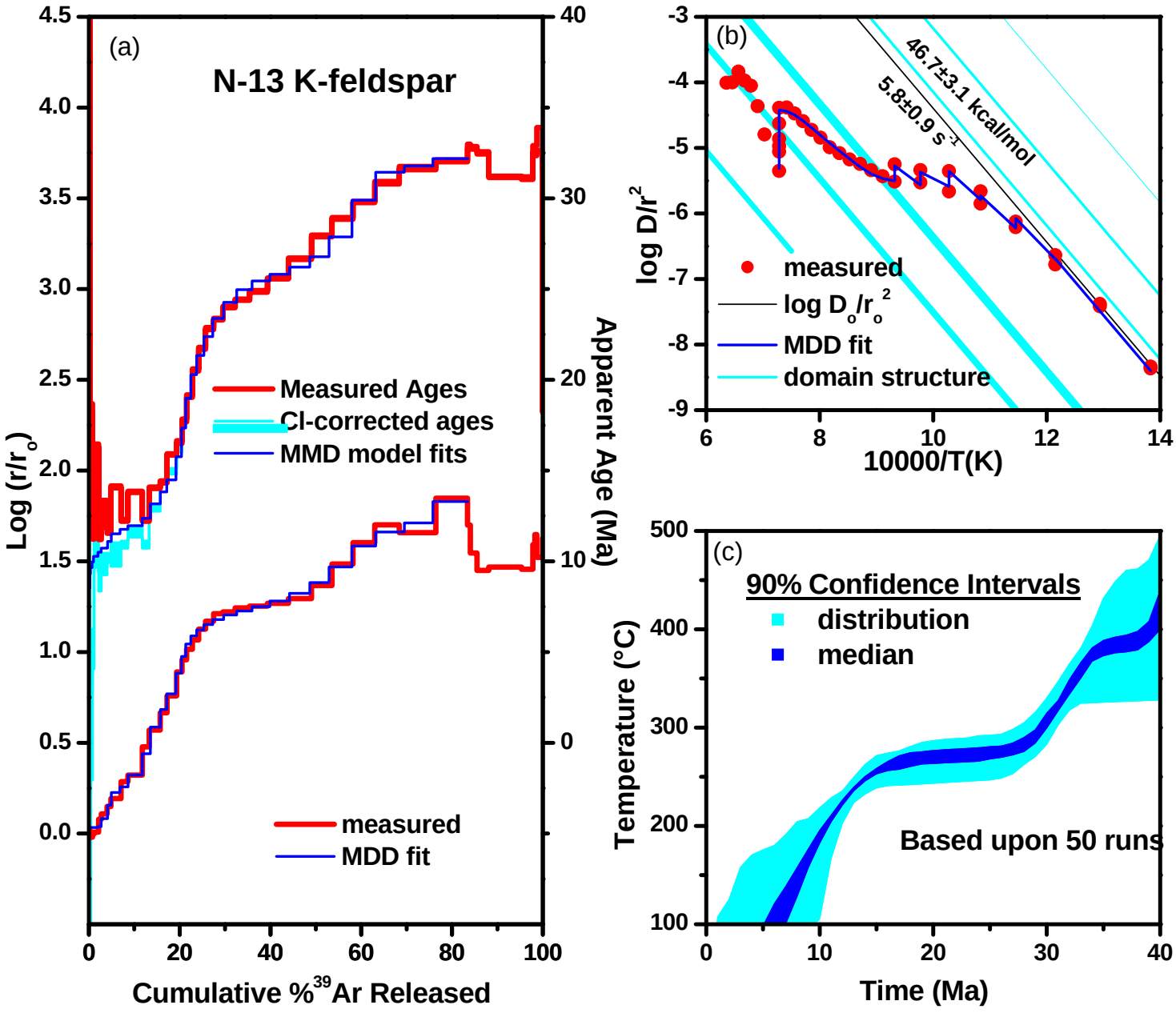
(a)
N-13 K-feldspar
Measured Ages
Cl-corrected ages
MMD model fits
measured
MDD fit
Log (r/r$_o$)
Apparent Age (Ma)
Cumulative %^{39}Ar Released
(b)
46.7±3.1 kcal/mol
5.8±0.9 s^{-1}
measured
log D$_o$/r$_o$^{2}
MDD fit
domain structure
log D/r^2
10000/T(K)
(c)
90% Confidence Intervals
distribution
median
Based upon 50 runs
Temperature (°C)
Time (Ma)

Figure 3

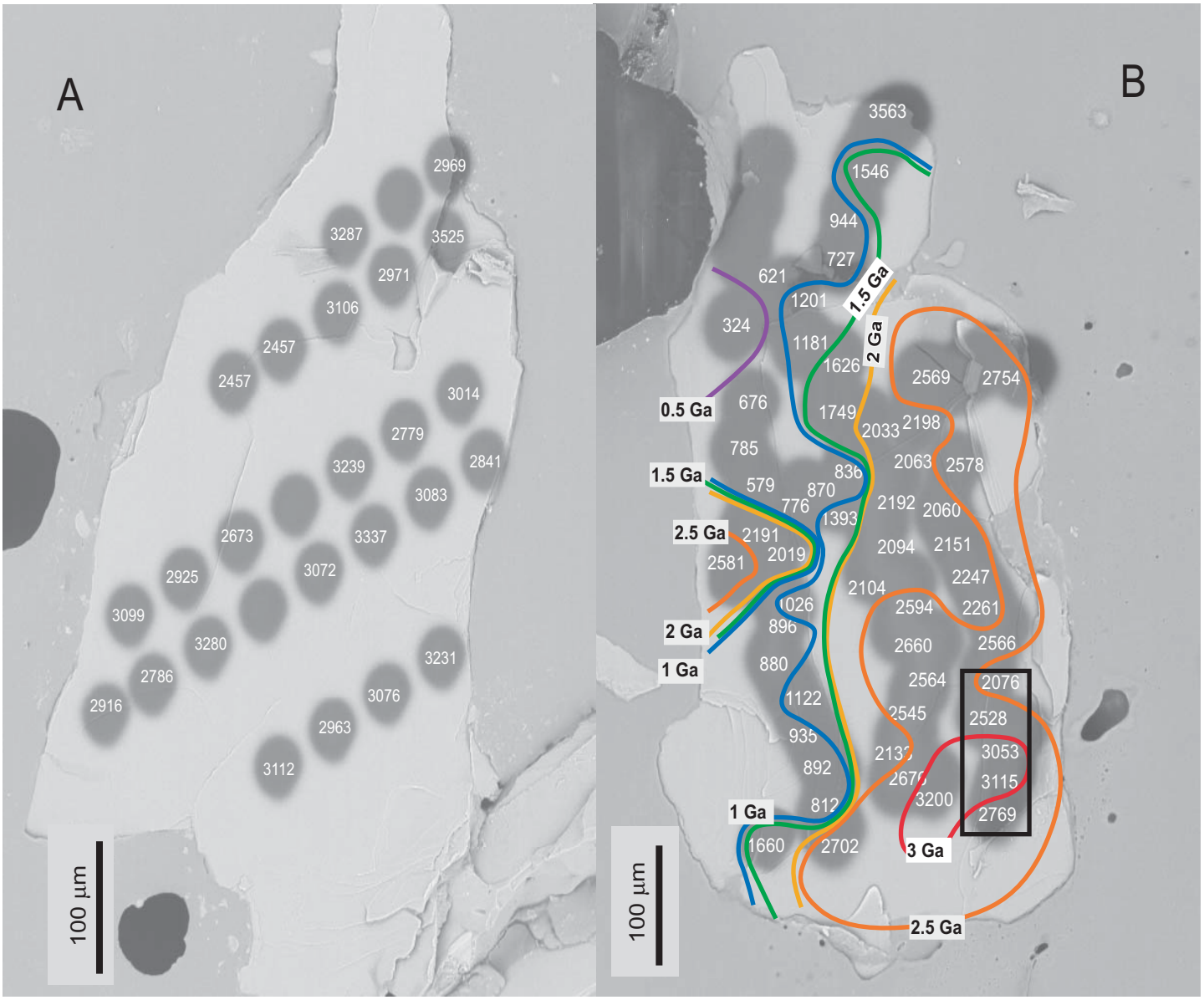
A
2969
3287
3525
2971
3106
2457
2457
3014
2779
2841
3239
3083
2673
3337
3072
2925
3099
3280
2786
3231
2916
3076
2963
3112
100 µm
B
3563
1546
944
727
621
1201
1.5 Ga
324
1181
2 Ga
1626
2569
2754
0.5 Ga
676
1749
2033
2198
785
836
2063
2578
1.5 Ga
579
870
776
1393
2192
2060
2.5 Ga
2191
2019
2581
2094
2151
2104
2247
1026
2594
2261
2 Ga
896
2660
2566
1 Ga
880
2564
2076
1122
2545
2528
935
3053
892
3115
812
3200
2769
1 Ga
1660
2702
3 Ga
2.5 Ga
100 µm

Figure 4

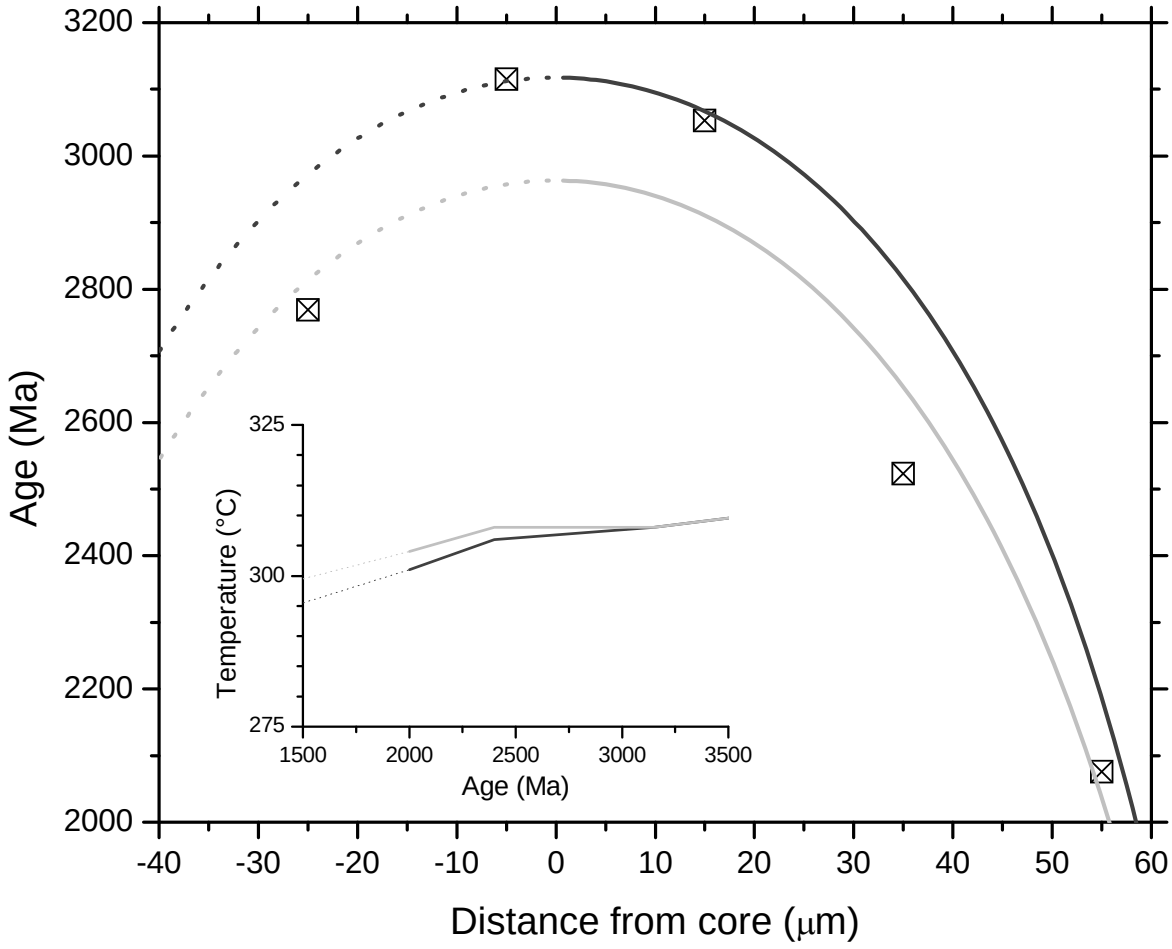
3200
3000
2800
2600
2400
2200
2000
Age (Ma)
-40
-30
-20
-10
0
10
20
30
40
50
60
Distance from core (μm)
325
300
275
Temperature (°C)
1500
2000
2500
3000
3500
Age (Ma)

Figure 5.

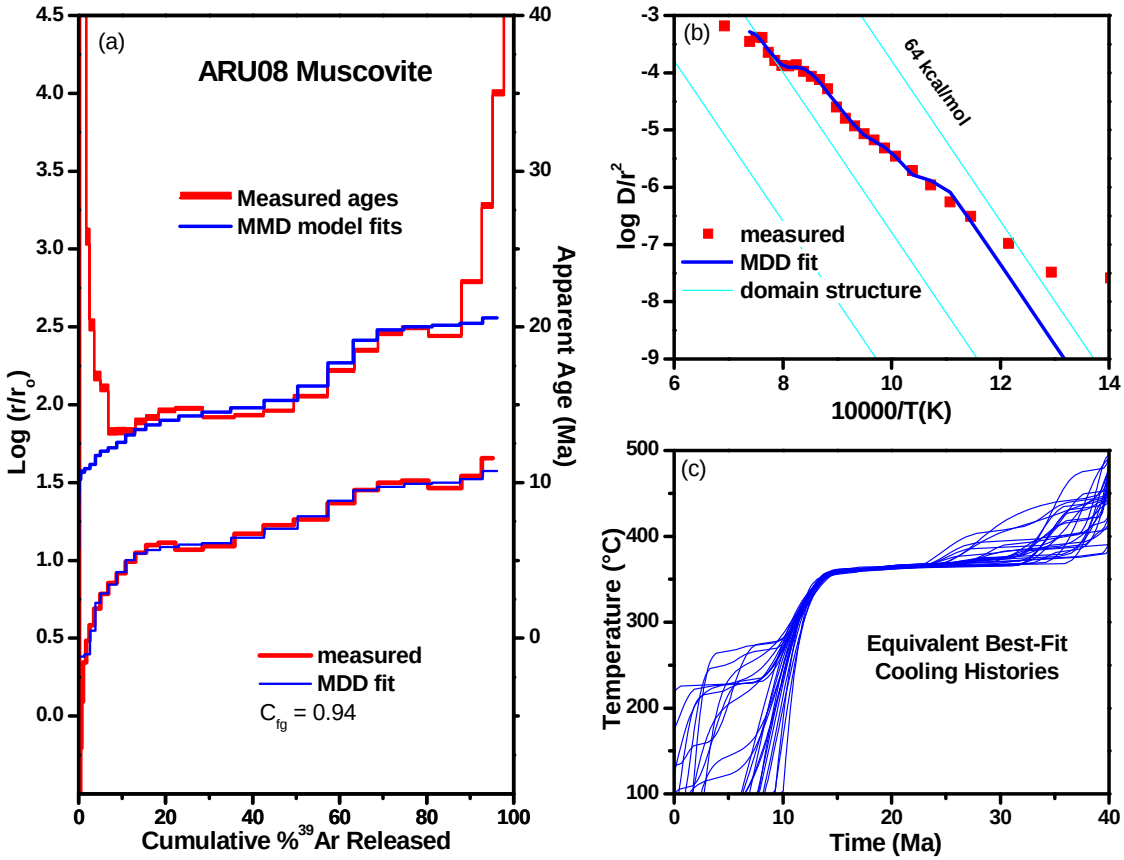
(a)
ARU08 Muscovite
Measured ages
MMD model fits
measured
MDD fit
C_fg = 0.94
Log (r/r_o)
Apparent Age (Ma)
Cumulative %39Ar Released
(b)
64 kcal/mol
measured
MDD fit
domain structure
log D/r^2
10000/T(K)
(c)
Equivalent Best-Fit
Cooling Histories
Temperature (°C)
Time (Ma)

Figure 6